Vol. 44, No. 2 (2022) 212-220, DOI: 10.24874/ti.1083.03.21.07

Tribology in Industry

www.tribology.rs

RESEARCH

Microstructure and Wear Resistance of Plasma Surface Layers Based of Alloy Mixture CuSn10/CrxCy

Andrey Evgenievich Balanovskiy[a,*], Van Trieu Nguyen[a], Natalia Anatolyevna Astafeva[a], Van Huy Vu[a]

[a]*National Research Irkutsk State Technical University, Russia.*

Keywords:

Microstructure
Wear resistance
Tin-bronze
OK 84.78
Microhardness
Chemical composition
Clad layer
Plasma heating

* Corresponding author:

Andrey Evgenievich Balanovskiy
E-mail: fuco.64@mail.ru

Received: 30 March 2021
Revised: 21 June 2021
Accepted: 22 July 2021

A B S T R A C T

The article relates to the study of the microstructure and wear resistance of the surface layers obtained by plasma heating of the powder-clad layer of the CuSn10 alloy and the coating of the OK 84.78 welding electrode. Microstructure studies, hardness measurements and wear tests have shown that coatings based on a tin-bronze alloy and with the addition of OK 84.78 are successfully obtained. Coating from CuSn10 + 20% alloy mixture OK 84.78 has a hardness of about 500-700 HV, and from CuSn10 alloy it is about 310-564 HV. Meanwhile, the wear resistance also increases in series: Steel St3 < coating (CuSn) < coating (CuSn + 20% OK 84.78).

1. INTRODUCTION

For most types of protective coatings, an increase in hardness, as well as wear resistance, is the main goal that ensures the performance of parts under operating conditions, especially in wear [1-3]. In fact, the use of metal coatings on a large scale as in industry, several functional factors need to be addressed, including between the properties achieved and the cost, the utilization rate of materials (CMM), between the technological methods and energy consumption, between the compatibility of the materials used and the cost of equipment. Etc. [2-5].

Recently, among modern methods, plasma technology is widely used for hardening the surface of metals and alloys as the plasma arc transfer, in especial, plasma heating with a non-consumable electrode in a protective gas has more often used in the research of protective coatings [3-5]. This method can be solve relatively several of the above factors such as low cost of equipment, high efficiency, CMM, short processing time and others [5,6]. The main problem in plasma processing is the melting of the substrate during processing, which strongly changes the structure and properties of the resulting surface layer with the difficulty of controlling the dilution factor of metals and alloys [6,7].

Copper-based coatings or its alloys are best for anti-fouling, reducing friction, but the low hardness of this type of coatings limits their use in more severe conditions such as high wear. In particular, the creation of multi-element coatings based on a copper alloy containing Fe, Cr, C and other alloyed elements is encountered with difficulty due to the low solubility of copper or its alloys in other matrices such as iron, and vice versa [8,9]. As a result, the coating turns out to be inhomogeneous and there are sublayers that differ in hardness and structure [9,10]. It is known that studies of the creation of coatings of the Fe-Cu-C/Fe-Cr-C-Cu/Fe-Cr-C-Cu-Sn system are presented using laser technology using the bronze alloy, an iron alloy and chromium, especially with a slight melting of the substrate [8-10]. The presence of chromium and iron in the composition increases the wear resistance, but little changes the coefficient of friction of the coating based on the Cu-Sn alloy [9]. In the case of coatings, it has also been shown that the type of Fe-Cu based coating provides higher corrosion resistance than carbon steel. Tin-bronze (CuSn) – copper alloy is used as materials for sliding bearings, due to their high thermal conductivity, electrical conductivity, excellent wear resistance and corrosion resistance, and the absence of pollution, but its coatings have low hardness [11,12]. It is known that chromium carbide is a potentially suitable ceramic phase for use in cermets due to the excellent resistance to oxidation of its three polymorphs - cubic ($Cr_{23}C_6$), hexagonal (Cr_7C_3) and rhombic (Cr_3C_2) [13]. Composites based on chromium carbide are widely used tribological materials in high-temperature applications requiring high resistance to wear and corrosion-oxidation [13-15]. It is known that chromium carbides are widely used in many industries due to their low cost, flexibility, and popularity. The low melting point helps to reduce the heat consumption during the melting process, and the proximity of the temperature coefficient of linear expansion is comparable to that of steels, leads to a decrease in stresses in the transition layer when coating a steel base [15-16]. Therefore, when approaching the creation of a coating of the Fe-Cr-C-Cu-Sn system, the combination of tin-bronze and chromium carbide (CrxCy) during plasma heating of their preliminary coating layer can lead to high uniformity due to their high solubility at high temperatures with little attention to substrate dilution.

The purpose of this work is to study the wear resistance of surface coatings obtained by plasma heating of a mixture of the CuSn10 alloy and the coating of the welding electrode OK 84.78. The results are presented by studying the microstructure, measuring the hardness, and studying the wear resistance in the wear test.

2. EXPERIMENT

The processed substrate is St3 steel (GOST 380-2005). The mixture for the preparation of the clad layer on the St3 surface consists of the PRV-BrO10 (CuSn10) alloy and the welding electrode coating OK 84.78 (ESAB) with the composition: 4.5% C, 1.2% Mn, 1.2% Si, 33% Cr. The particle size of the PRV-BrO10 alloy is in the range of 10-150 microns. The particle size of the powder coating of the welding electrode OK 84.78 after grinding is in a wide range of 2-300 microns. The clad layer was prepared by mixing a mixture of PRV-BrO10 powder, OK 84.78 coating with silicate glue, then dried at 373 K for 1 hour. Plasma heating of the pre-coated sample surface is shown in fig. 1.

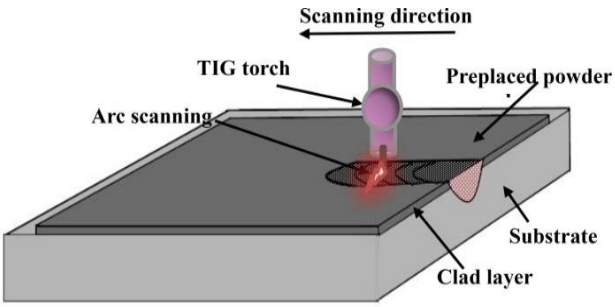

Fig. 1. Model of scanning an electric arc on a metal surface with a preliminary powder clad layer (pre-coating).

The device described in detail in the work [5] was used as a source of plasma heating. Plasma processing was performed on a setup that includes a Kempi PSS5000 power supply, a TU50 oscillator (TU50 control unit), a C110D remote control, an MU10 digital analyzer (for reading current and voltage values), a WU10 cooling system, a plasma-forming gas cylinder (argon), Kemppi TX163GS4 welding torch and tripod. Tungsten electrode with a diameter of 2.0mm. The stand is equipped with clamping devices that allow you to fix the torch and change the height of the arc gap. Also, the installation consists of a mechanism for moving samples.

The stage is equipped with special clamping elements for fixing previously prepared sample fragments on it. The movement of the table is carried out using an electric drive that operates from a 24 V power source. The speed control of the stage is carried out using a potentiometer. The potentiometer creates resistance and reduces the voltage, and therefore the speed of the stage. The table travel speed ranges from 5.4 to 39.6 m/h. As recommended, for surfacing of the welding electrode OK 84.78 in a power of 110-170 A, therefore, the used plasma heating mode: average power – current strength 140 A; the speed of movement of the samples is 2.7 mm/s; gas (argon) feed rate 10 l/min, the distance between the clad layer (pre-coating) and the electrode is 5-7 mm. It is known that the melting point of CuSn10 is low, about 1273 K [17], and for chromium carbides it is 1800-2200 K [18], therefore, two modes are applied for each mixture shown in Table 1. After cutting, polishing and etching the obtained samples, their microstructures were studied using a MET-2 metallographic microscope, and the hardness of the coatings was measured using the HMV-G21 microhardness tester. The study of the microstructure of coatings and steel is given on a metallographic microscope of the MET-2 brand. The chemical composition of the coatings is performed on a JIB-4500 microscope with an EDS analyzer and an ARC-MET 8000 analyzer.

Table 1. Composition and parameters for processing samples.

№	1	2
Composition	CuSn10	CuSn10 + 20%OK 84.78
Thickness of clad layer	0,50 mm	0,25 mm
The gap between the pre-coating and the electrode	7 mm	5 mm
Cooling type	Water	Air

3. RESULTS AND DISCUSSION

The obtained coatings are represented by the microstructure and the distribution of the hardness of the cross-section shown in figures 2, 3, 4. It can be seen from them that there is a difference between the two types of coatings: only CuSn10 and CuSn10 with CrxCy in the form of OK 84.78 coating. In the case of the coating based on CuSn10, it is noted that the distribution of hardness values is in a wide range due to the uneven arrangement of phases rich in bronze (bright) or iron (dark). In the upper part (fig. 2 a), the main structures of the dark zones are cellular and columnar, in the lower part there are cracks (Fig. 2 b). In the central region, bright zones occupy a large area, represented by a length and width of several hundredths of a micrometer. The hardness of the point falling on the bright zone is 229 HV, and for the point on the dark zone of the crack – 134 HV, for the rest of the measured points in the range 310 – 564 HV. In the case of the coating on a mixture of CuSn10 and 20% OK 84.78, it is noted that the presence of CrxCy in the composition significantly affects the change in the structure and hardness in comparison with a coating based on CuSn10.

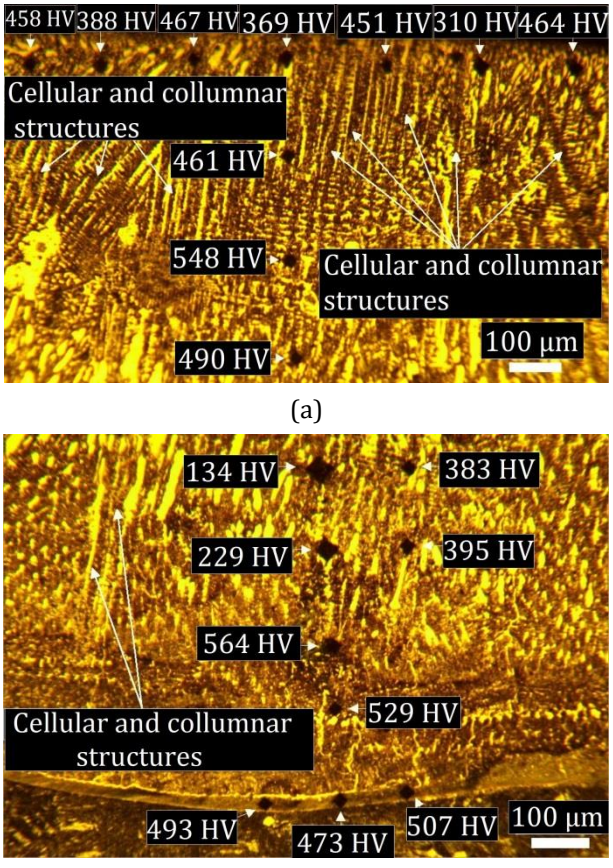

Fig. 2. Distribution of hardness in depth from the surface in the central region of the coating based on CuSn10 alloy: (a) - upper part, (b) - lower part.

The addition of CrxCy results in a reduction in the bright areas rich in bronze. In fig. 3 is shown that the main structures are not only cellular and columnar, but also equiaxed. Hardness

values are in the range of 464 - 673 HV, i.e. the presence of CrxCy increases the minimum hardness by 100 HV. In the left edge of the coating based on a mixture of CuSn10 + 20% OK 84.78, it can be seen that, on the outside of the surfacing bath, the alloyed layer continues to a few hundredths of a micrometer with a decrease in hardness along the distance from the boundary (in Fig. 4 a). In the zone of the left edge inside the surfacing bath, the hardness is very high (577 - 707 HV), and for the zone of the left edge of the external surfacing bath, the hardness decreases to 186 HV (in Fig. 4 b, c).

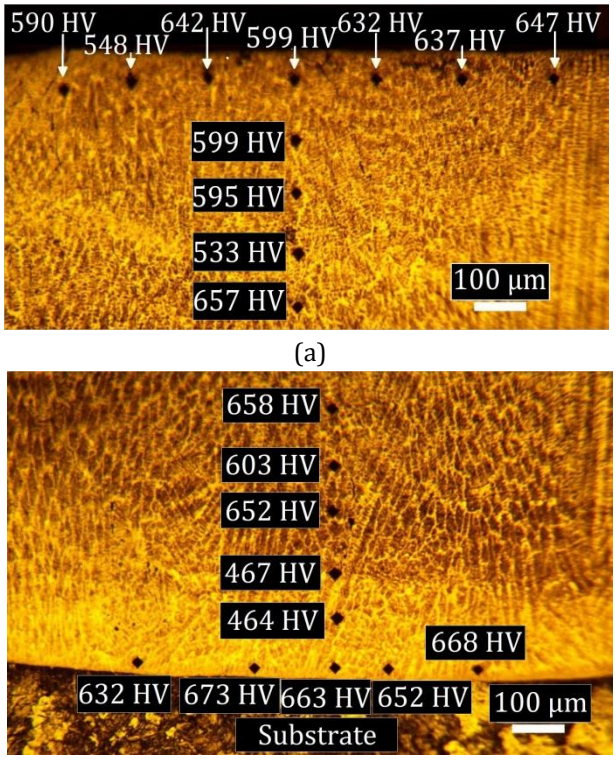

Fig. 3. Distribution of hardness in depth from the surface in the central region of the coating based on the CuSn10 + 20% OK 84.78 alloy: (a) upper part, (b) lower part.

The chemical composition is given in depth from the coating surface in Figure 5-a. The selected spectra are characterized for three main zones: copper-rich; rich in iron and heat affected. Spectrum 1 showed that tin and copper are the main elements, i.e. CuSn10 plays a role as a matrix. In spectrum 3, the main element is iron; there is little copper and no tin, which means a low solubility of bronze in steel in the lower zone. The absence of tin and copper in the heat-affected zone is noted that there is no diffusion of bronze beyond the boundary between the main coating and the substrate.

Consideration of the chemical composition in the central region has shown by spectra 1, 2 in Fig. 5-b. The presence of tin, copper and iron again suggested that the solubility of iron in bronze is low, but on the contrary, bronze dissolves slightly in iron. The difference in the chemical composition of the local zones is already represented by the hardness values given in Fig. 2.

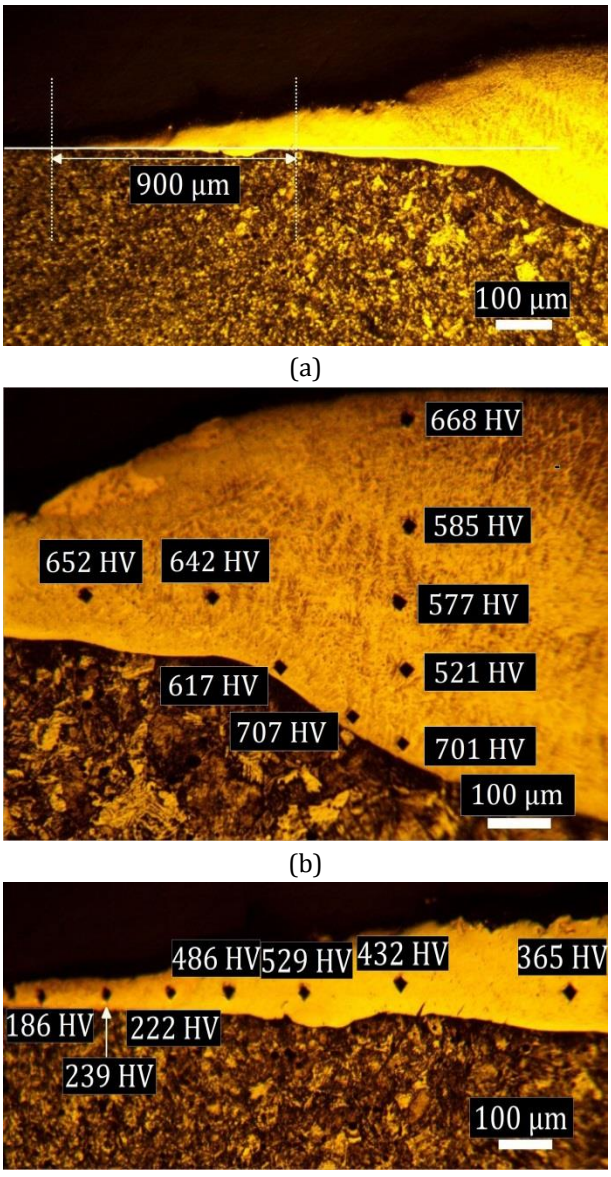

Fig. 4. Formation of the left edge of the coating with a hardness distribution based on the CuSn10 + 20% OK 84.78 alloy; (a) - left edge, (b) - zone of the left edge inside the surfacing bath, (c) - the zone of the left edge of the external surfacing bath.

From the chemical composition of the spectra 1, 2 (Fig. 5), the type of coating as a dispersion system between bronze and iron. In Figure 6,

the distribution of structures is clearer, which are where based on the iron phase and vice versa based on CuSn10. Several spectra show that tin is absent in the iron matrix, and copper is not strongly soluble in it. According to the phase diagram of the Fe-Cu system, at high temperatures, primary γ-Fe dendrites can form as a result of a liquid-solid transformation and then solidify at 1693 K. Then, due to liquid-phase separation, a copper-rich liquid matrix (L) is formed, and further cooling leads to a peritectic transformation at 1356 K according to the reaction 1 [19]:

$$L + \gamma - Fe \rightarrow \varepsilon - Cu + \alpha - Fe \quad (1)$$

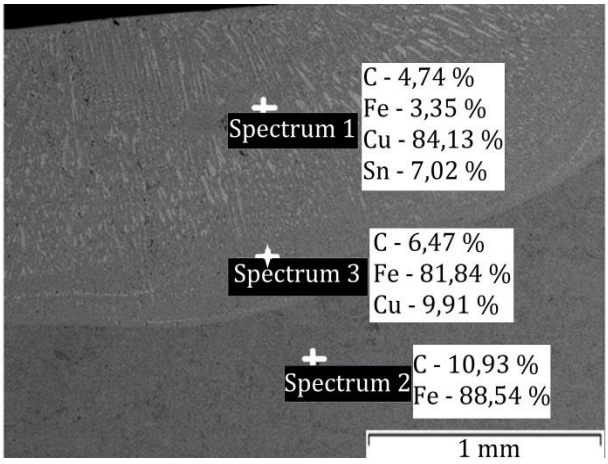

(a)

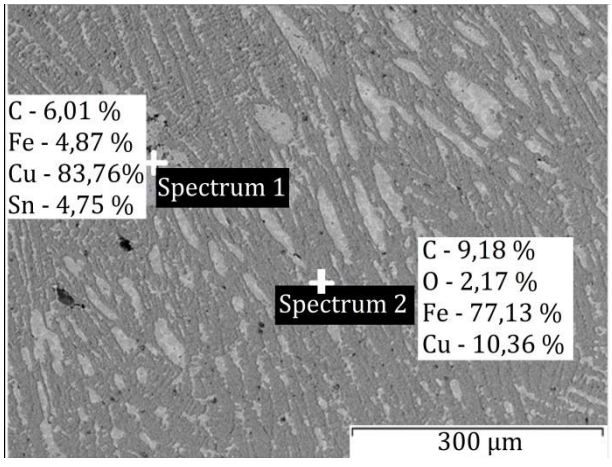

(b)

Fig. 5. The result of determining the chemical composition of the coating based on the PRV-BrO10 alloy.

This means that in the iron-rich zone, the phase constituents mainly consist of α-Fe and ε-Cu, while the rich Cu phases can be α (Cu, Sn), Cu10Sn3 and Cu41Sn11.

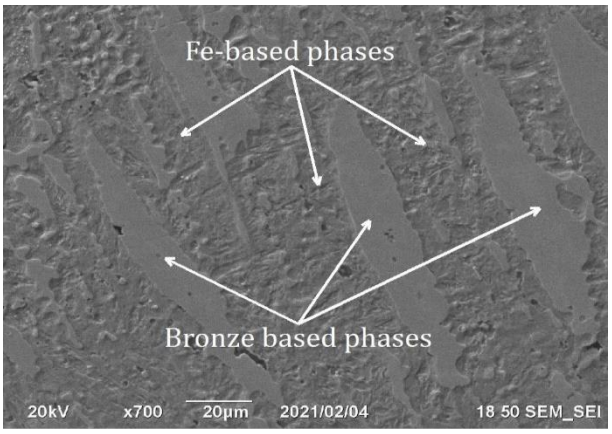

Fig. 6. Microstructure of the central zone of the surface layer of the Fe-C-Cu-Sn system.

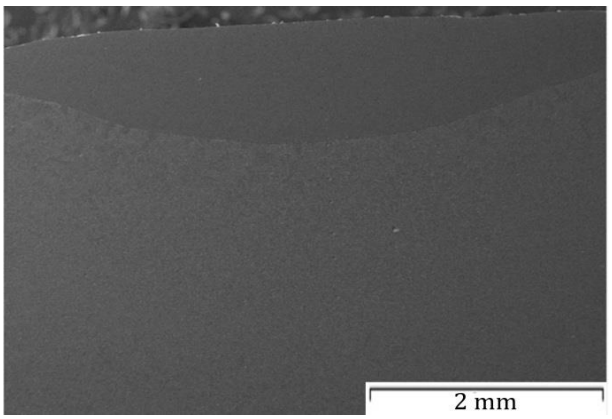

Fig. 7. Cross-section of the coating based on the alloy CuSn10+20%OK 84.78.

The determination of the chemical composition of the surface layer of the 20% OK 84.78 type of coating is given in Table 2. As shown, the cross-section of the coating based on mixture of CuSn10 and 20% OK 84.78 in Fig. 3. The surfacing pool is uniform and the depth is more than a millimeter. The dilution factor of the substrate is 51% (Fig. 7). It is known that the thickness of the clad layer is fixed at 0.25 mm, and the depth of the coating is about 1 mm, four times more. Therefore, this is consistent with the results shown in table 2 with a high iron content. The composition is given as for alloy steel.

Table 2. The total number of main elements in the coating CuSn10/CrxCy.

Element	Total spectrum
C	13.39
O	3.46
Cr	0.61
Fe	77.42
Cu	3.79
Sn	0.37
Si	0,15
Mn	0,47

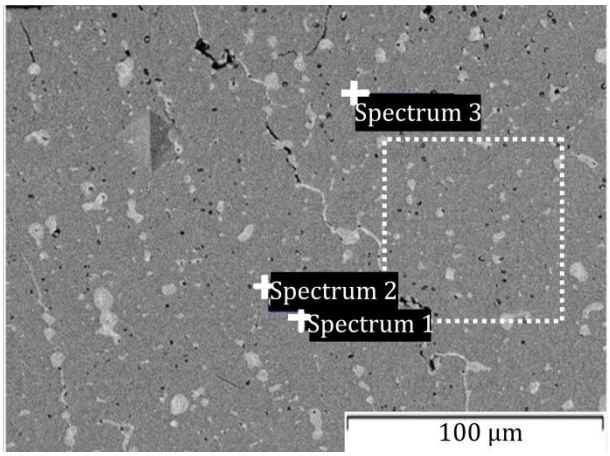

(a)

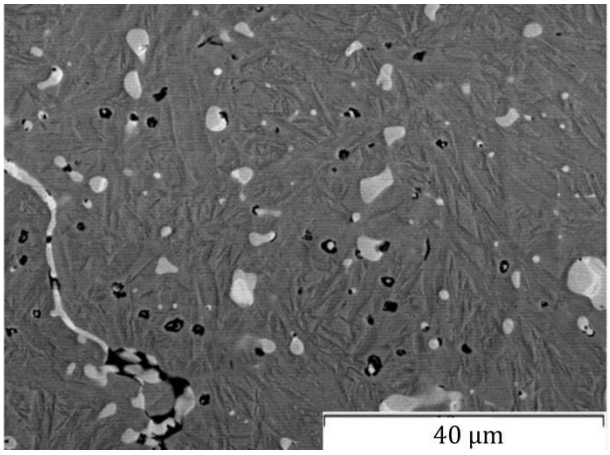

(b)

Fig. 8. Cross-section of the central zone of the surface layer based on the alloy CuSn10+20%OK 84.78.

Table 3: Total number of main elements in some considered spectra.

Spectrum	1	2	3
Fe	5.44	77.77	65.67
Cr	0.14	2.32	2.06
C	10.10	7.52	5.85
O	0.80	1.04	0.80
Cu	75.17	9.52	19.89
Sn	7.42	0.20	3.99
Si	0,09	0,18	0,20
Mn	0,55	0,36	0,54

Study of the central zone (in Fig. 8) showed that there are microcracks filled with bronze. The area of the bronze-rich zones has already been reduced compared to a CuSn-only coating. The solubility of bronze in the iron matrix is already better with the addition of chromium carbide, represented by the chemical composition in the spectra 1,2,3 (in Fig. 8-a and Table 3). Fig. 8b shows the dotted area from Fig. 8a showing round bronze-rich particles distributed on an iron-rich matrix with a martensite structure.

It is also seen from table 3 that chromium dissolves better in bronze due to high temperatures during the heating process, respectively, with the concept of its solubility in the copper matrix [20].

It is known that Cu and Sn do not form carbides, while Fe, Cr can combine with carbon according to the following reactions 2, 3:

$$23(Fe, Cr) + 6C \rightarrow (Fe, Cr)_{23}C_6 \quad (2)$$

$$7(Fe, Cr) + 3C \rightarrow (Fe, Cr)_7C_3 \quad (3)$$

According to these compositions, the OK 84.78 coating contains manganese, which can form carbides together with iron and chromium: $(Fe, Cr, Mn)_3C$, $(Fe, Cr, Mn)_7C_3$ $(Fe, Cr, Mn)_{23}C_6$ [21].

In fig. 9 shows the distribution of chemical elements in the square dashed area (Fig. 8 - b), and table 4 shows their content. The presence of iron is shown by a red background and presence of other alloying elements with different colors. The distribution of tin-bronze is again shown by the distribution of Cu and Sn, clearly having the same distribution region. Tin-bronze is located more in cracks and in round zones.

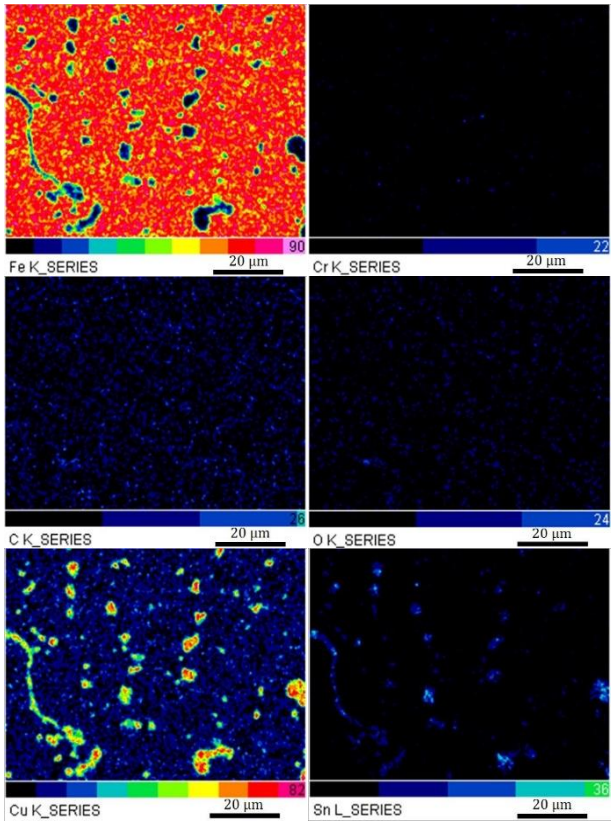

Fig. 9. Distribution of chemical elements in the cross section of the alloyed coating.

Table 4. Total number of main elements of considered zone.

Element	Total spectrum
C	5.67
O	1.65
Cr	2.35
Fe	73.08
Cu	14.23
Sn	1.33
Si	0,25
Mn	0,49

High carbon content does not mean from the original composition, but maybe from contaminated resources in the environment. Therefore, the distribution of carbon can be seen in the entire field of view (dark blue). The presence of oxygen and chromium is lower than that of other elements with a dark blue distribution. The presence of oxygen is associated with the oxidation of metals by the adhesive containing it in the silicate formula. The formula for liquid glass $Na_2O{\cdot}mSiO_2{\cdot}nH_2O$ recommends that the silicon content is small, and the oxygen is much, but after drying the pre-coating, the water groups were driven away from the mixture, the rest of the oxygen content during the plasma heating process either combines with metals, forming welding slags on the surface of the coatings [5,6].

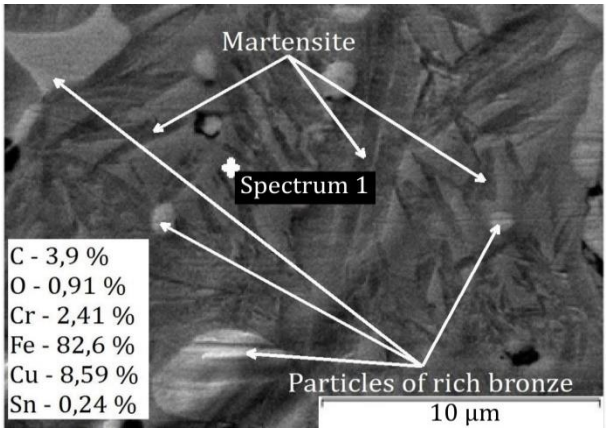

Fig. 10. Typical zone with martensite and rich bronze particles.

The distribution of the phase and chemical composition of a small zone is shown in Figure 10. In this zone, unmixed particles of rich bronze remain, and around them, there are martensitic phases, as well as pores less than 2 μm in size. As in a coating of the CuSn type, in a coating of the CuSn10 + 20% OK 84.78 type not only α-Fe and ε-Cu exist, rich Cu phases can be α (Cu, Sn), $Cu_{10}Sn_3$ and $Cu_{41}Sn_{11}$, but also carbide phases in the form $(Fe , Cr)_{23}C_6$, $(Fe, Cr)_7C_3$ and the Fe-rich spheroid consists of γ (Fe).

The results of the distribution of individual coating elements of coating CuSn10 + 20% OK 84.78 showed that the high power of the plasma jet provides sufficient heat to dissolve the alloy mixture and a part of the substrate. This improves the uniformity of the coating better than coatings treated with other sources [22,24,26]. Further, it was found that the resulting coating has a higher hardness compared to coatings obtained from a typical composition by laser and spraying (thermal and cold) treatment, having a hardness below 500 HV [24-26].

Table 5 shows the values of the microhardness of the coatings, the heat-affected zone and the base steel St3. The results of the wear test are represented by the mass loss shown in Figure 11. First, the test mode was set up with SiC 220 sandpaper, load of 50 N, rotation speed of the aluminum plate 500 rpm, holder speed 150 rpm with reverse rotation, water-cooling. The weight loss increases in the following order: coating (CuSn10 + 20% OK 84.78) <coating (CuSn10) <Steel St3. This is, respectively, with the difference in hardness, i.e. by adding chromium carbide. With high grain size, i.e. small particles, the rate of weight loss of the two types of coatings is slow within an hour and a half.

Table 5. Characteristics of the test samples.

Initial composition	CuSn10	CuSn10+20 % OK 84.78	Steel St3
Thickness of coating, μm	1300	1090	-
Hardness of coating, HV	300-564	500-700	140-160
Hardness of heat affected zone (HAZ), HV	170-200	170-210	

To speed up the abrasion process, the test mode was rebuilt with a waterproof sanding paper Dexter P80, a load of 50 N, an aluminum plate rotation speed of 400 rpm, a holder speed of 150 rpm with reverse rotation, water cooling. The change in grain size greatly affects the loss of mass, as a result of which the wear process reaches the base steel faster. For half an hour, the rate of weight loss is several times greater than in the first case. This increase is due to the low hardness of

the heat-affected zone to which the wear process reaches. In the second case (Fig. 11 b), between the two coatings, the weight loss does not differ significantly, perhaps because the depth of the CuSn10 coating is greater than that of the CuSn10 + 20% OK 84.78 coating.

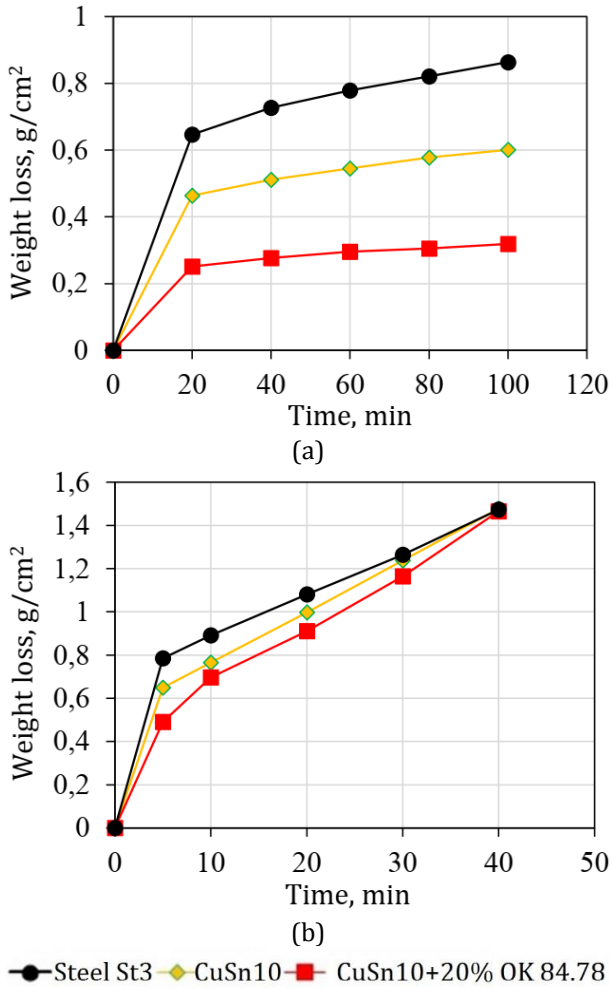

Fig. 11. Weight loss of samples under load 50 N; (a) 220 SiC sandpaper, load 50 N, aluminum plate speed 500 revs/min, holder speed 150 revs/min, counter-rotation, water; (b) - grinding water-resistant Dexter P80, load 50 N, speed of the aluminum plate 400 revs/min, holder speed revs/min, counter-rotation, water.

4. CONCLUSIONS

It was found that upon plasma heating of a clad layer of CuSn10, CuSn10 + 20% OK 84.78 alloys, surface layers were successfully obtained on St3 steel. It is noted that the addition of CrxCy strongly changes the hardness of the cross-section of the coatings, in which, for the CuSn10 + 20% OK 84.78 type, it is in the range of 500-700 HV, and for the CuSn type, from 310 to 564 HV.

The study of the microstructure and chemical composition revealed that the presence of CrxCy leads to the addition of hard phases to the matrices of copper and iron. As a result, the main phase composition can be composed of α-Fe, γ (Fe), ε-Cu, α-(Cu, Sn), $Cu_{10}Sn_3$, $Cu_{41}Sn_{11}$, $(Fe, Cr)_{23}C_6$, $(Fe, Cr)_7C_3$.

The wear test showed that the weight loss decreases in the following order: coating (CuSn + 20% OK 84.78) <coating (CuSn) <Steel St3, and a coating of the CuSn + 20% OK 84.78 type has the best wear resistance.

REFERENCES

[1] P. Hvizdoš, *Wear and Erosion Resistant Ceramic Materials*, Encyclopedia of Materials: Technical Ceramics and Glasses, Elsevier, vol. 2, pp. 416-424, 2021, doi: 10.1016/B978-0-12-818542-1.00056-4

[2] M.N. Brykov, V. Efremenko, *Abrasive Wear Resistance of Steels and Cast Irons*, Herson: Grin D.S., 2014, doi: 10.13140/2.1.1395.7129 (in Russian)

[3] A.P. Thummar, S.P. Wanare, V.D. Kalyankar, *Effect of Dilution on Microstructure and Slurry Abrasive Wear Behaviour of Ni-Cr-Mo-W Coating on 304 Stainless Steel Deposited by Synergic Pulsed Gas Metal Arc Welding*, Tribology in Industry, Articles in Press, pp. 1-14, 2021, doi: 10.24874/ti.984.10.20.01

[4] V.H. Vu, A.E. Balanovskiy, V.T. Doan, V.T. Nguyen, *Surface Saturation with Carbon Using Plasma Arc and Graphite Coating*, Tribology in Industry, vol. 43, no. 2, pp. 211-221, 2021, doi: 10.24874/ti.951.08.20.12

[5] A.E. Balanovskiy, V.H. Vu, *Saturation of the metal surface with carbon during plasma surface treatment*, Hardening technologies and coatings, no. 9, pp. 403-415, 2017. (in Russian)

[6] A.E. Balanovskiy, V.H. Vu., *Plasma surface carburizing using a graphite coating*, Materials Letters, vol. 7, No. 2 (26), pp. 175-179, 2017, doi: 10.22226/2410-3535-2017-2-175-179

[7] G.P. Rajeev, M. Kamaraj, R.B. Srinivasa, *Comparison of microstructure, dilution and wear behavior of Stellite 21 hardfacing on H13 steel using cold metal transfer and plasma transferred arc welding processes*, Surface and Coatings Technology, vol. 375, pp. 383-394, 2019, doi: 10.1016/j.surfcoat.2019.07.019

[8] X. Dai, S. Zhou, M. Wang, J. Lei, M. Xie, H. Chen, C. Wang, T. Wang, *Effect of substrate types on the microstructure and properties of Cu65Fe35 composite coatings by laser induction hybrid cladding*, Journal of Alloys and Compounds, vol. 722, pp. 173-182, 2017, doi: 10.1016/j.jallcom.2017.06.064

[9] Q.Y. Hou, T.T. Ding, Z.Y. Huang, Pi. Wang, L.M. Luo, Y.C. Wu, *Microstructure and properties of mixed Cu–Sn and Fe-based alloys without or with molybdenum addition processed by plasma transferred arc*, Surface and Coatings Technology, vol. 283, pp. 184-193, 2015, doi: 10.1016/j.surfcoat.2015.10.043

[10] S. Zhou, J. Lei, Z. Xiong, X. Dai, J. Guo, Z. Gu, *Synthesis of Fep/Cu-Cup/Fe duplex composite coatings by laser cladding*, Materials & Design, vol. 97, pp. 431-436, 2016, doi: 10.1016/j.matdes.2016.02.125

[11] C. Paul, R. Sellamuthu, *The Effect of Sn Content on the Properties of Surface Refined Cu-Sn Bronze Alloys*, Procedia Engineering, vol. 97, pp. 1341-1347, 2014, doi: 10.1016/j.proeng.2014.12.414

[12] J. Freudenberger, H. Warlimont, *Copper and Copper Alloys*, Springer Handbook of Materials Data, pp. 297-305, 2018, doi: 10.1007/978-3-319-69743-7_12

[13] R.D. Laranjo, *Thermodynamic analysis in the production of chromium carbide from the reduction of chromium oxide with methane-containing gas*, International Journal of Engineering and Techniques, vol. 4, iss. 2, pp. 227-232, 2018.

[14] M. Antonov, I. Hussainova, *Cermets surface transformation under erosive and abrasive wear*, Tribology International, vol. 43, iss. 8, pp. 1566-1575, 2010, doi: 10.1016/j.triboint.2009.12.005

[15] A. Zikin, I. Hussainova, C. Katsich, E. Badisch, C. Tomastik, *Advanced chromium carbide-based hardfacings*, Surface and Coatings Technology, vol. 206, iss. 19-20, pp. 4270–4279, 2012, doi: 10.1016/j.surfcoat.2012.04.039

[16] A. Ganguly, M. Vinuthaa, K. Kannoorpatti, *Structural and electronic properties of chromium carbides and Fe-substituted chromium carbides*, Materials Research Express, vol. 7, no. 5, pp. 1-13, 2020, doi: 10.1088/2053-1591/ab8cf9

[17] R. Konečná, S. Fintová, *Copper and Copper Alloys: Casting, Classification and Characteristic Microstructures, Copper Alloys - Early Applications and Current Performance - Enhancing Processes*, InTech, 2012, doi: 10.5772/39014

[18] D.D.L. Chung, *7 - Carbon-Matrix Composites*, *Carbon Composites (Second Edition),* in Carbon Composites, Composites with Carbon Fibers, Nanofibers and Nanotubes, Butterworth-Heinemann, pp. 387-466, 2017, doi: 10.1016/B978-0-12-804459-9.00007-5

[19] J.T. Zhang, X.C. Cui, Y.T. Yang, Y.H. Wang, *Solidification of the Cu-35 wt pct Fe alloys with liquid separation*, Metallurgical and Materials Transactions A, vol. 44, pp. 5544-5548, 2013, doi: 10.1007/s11661-013-1905-6

[20] Q. Zhao, Z. Shao, C. Liu, M. Jiang, X. Li, R. Zevenhoven, H. Saxén, *Preparation of Cu-Cr alloy powder by mechanical alloying*, Journal of Alloys and Compounds, vol. 607, pp. 118-124, 2014, doi: 10.1016/j.jallcom.2014.04.054

[21] V.V. Netrebko, *Features of alloying of white wear-resistant cast irons,* Casting and metallurgy, no. 2, pp. 37-41, 2014. (in Russian)

[22] X. Dai, S. Zhou, M. Wang, J. Lei, C. Wang, T. Wang, *Microstructure evolution of phase separated Fe-Cu-Cr-C composite coatings by laser induction hybrid cladding*, Surface and Coatings Technology, vol. 324, pp. 518-525, 2017, doi: 10.1016/j.surfcoat.2017.06.032

[23] Y. Yang, A. Wang, D. Xiong, Z. Wang, D. Zhou, S. Li, H. Zhang, *Effect of Cr content on microstructure and oxidation resistance of laser-clad Cu-Ni-Fe-Mo-xCr alloy coating*, Surface and Coatings Technology, vol. 384, 125316, 2020, doi: 10.1016/j.surfcoat.2019.125316

[24] S. Zhou, X. Dai, M. Xie, S. Zhao, T.B. Sercombe, *Phase separation and properties of Cu-Fe-Cr-Si-C immiscible nanocomposite by laser induction hybrid cladding*, Journal of Alloys and Compounds, vol. 741, pp. 482-488, 2018, doi: 10.1016/j.jallcom.2018.01.184

[25] W. Chen, Y. Yu, A.K. Tieu, J. Hao, L. Wang, S. Zhu, J. Yang, *Microstructure, mechanical properties and tribological behavior of the low-pressure cold sprayed tin bronze-alumina coating in artificial seawater*, Tribology International, vol. 142, Available online, 2020, doi: 10.1016/j.triboint.2019.105992

[26] K.S. Al-Athel, M. Ibrahim, A.F.M. Arif, S.S. Akhtar, *Effect of Composition and Thickness on the Hardness and Scratch Resistance of Copper and Copper Alloy Coatings*, Arabian Journal for Science and Engineering, vol. 42, pp. 4895–4904, 2017, doi: 10.1007/s13369-017-2661-5